Enhanced Miscibility of Low-Molecular-Weight Polystyrene/Polyisoprene Blends in Supercritical CO_2

Teri A. Walker,[†] Srinivasa R. Raghavan,[†,||] Joseph R. Royer,[†] Steven D. Smith,[‡] George D. Wignall,[§] Yuri Melnichenko,[§] Saad A. Khan,[†] and Richard J. Spontak*[,†]

Department of Chemical Engineering, North Carolina State University, Raleigh, North Carolina 27695, Corporate Research Division, The Procter & Gamble Company, Cincinnati, Ohio 45239, and Solid State Division, Oak Ridge National Laboratory, Oak Ridge, Tennessee 37831

Received: February 15, 1999; In Final Form: April 20, 1999

While ongoing efforts continue to explore the high-pressure phase equilibria of polymer blends, few studies have attempted to address the impact of a supercritical (sc) fluid on such equilibria. In this work, we report on the phase behavior of an upper critical solution temperature (UCST) polymer blend in the presence of supercritical carbon dioxide ($scCO_2$), a nonselective plasticizing agent. Blends composed of low-molecular-weight polystyrene and polyisoprene have been examined as a function of temperature in $scCO_2$ by visual inspection, small-angle neutron scattering, and spectrophotometry. In the presence of $scCO_2$, the cloud point temperature is depressed by as much as 28 °C, depending on both blend composition and CO_2 pressure. Complementary studies performed with nitrogen decouple the plasticization efficacy of CO_2 from free-volume compression due to hydrostatic pressure. Existence of a pressure yielding a maximum in CO_2-induced cloud point depression is established. These results provide evidence for enhanced polymer miscibility as a result of the plasticizing effectiveness and tunable solubility of $scCO_2$.

Introduction

Polymers by their chainlike nature tend to be immiscible due to their generally low entropy of mixing and typical athermal or endothermic mixing.[1−3] In the absence of specific interactions between the constituent polymer species,[4] two general types of blends can be classified on the basis of the temperature dependence of the Flory−Huggins interaction parameter (χ). If χ decreases monotonically with increasing temperature, as is the case for most blends of commercial relevance, then the blend exhibits an upper critical solution temperature (UCST). In this case, a UCST blend of given composition remains miscible at high temperatures (insofar as it does not decompose) and generally phase-separates via nucleation and growth upon cooling below the binodal, or cloud point, temperature (T*). Some blends, on the other hand, exhibit the reverse, or lower critical solution temperature (LCST), behavior if χ increases monotonically with temperature, and the blend phase-separates upon heating above T*. A small number of polymer blends possess multiple critical solution temperatures.

The ability to alter, in tunable fashion, the miscibility of polymer blends is highly desirable, since it could expand the window of processability. While miscibility tuning is achievable through the use of organic solvents, this route is not environmentally benign and may require the use of hazardous chemicals. An emerging alternative to organic solvents in applications ranging from polymer synthesis[5−7] to polymer processing[8−10] is high-pressure carbon dioxide. Watkins et al.[11] have recently provided encouraging evidence that supercritical carbon dioxide ($scCO_2$) can be used to shift the phase boundaries of block copolymers, while Bungert et al.[12] have shown that $scCO_2$ has a significant effect on T* of a polystyrene−cyclohexane solution. These results differ from those reported for polymers subjected to hydrostatic pressure alone, which tends to decrease the miscibility of UCST blends,[13] but increase the miscibility of LCST blends.[14] Since $scCO_2$ serves as a plasticizing agent for polymer melts,[15−17] it follows that $scCO_2$ may reduce unfavorable interactions between two polymers, each interacting marginally with $scCO_2$, by increasing their free volume.[18] This would subsequently enhance their compatibility and shift their phase boundary in the direction of greater miscibility, which for a UCST system is accompanied by a reduction in T*. In the present work, we explore the competing effects of $scCO_2$ plasticization and hydrostatic pressure on the miscibility of a short-chain polymer blend exhibiting UCST behavior.

Experimental Section

Materials. Homopolystyrene (PS) with a number-average molecular weight ($\bar{M}_n$) of 3300 and a polydispersity index (PDI) of 1.09 was purchased from Aldrich Chemicals. Homopolyisoprene (PI) with $\bar{M}_n$ =1000 and PDI < 1.05 was synthesized via living anionic polymerization in cyclohexane at 60 °C in the presence of *sec*-butyllithium. The molecular weight characteristics of these materials, measured by GPC, were selected so that their theoretical phase diagram (Figure 1) coincided with both the range of $scCO_2$ processability and the operating limits of existing equipment. The polymers were melt-mixed at ca. 100 °C for visual experiments and at ca. 120 °C for small-angle neutron scattering (SANS) experiments. Two blends with PS weight fractions (w_S) of 0.20 and 0.36 were subjected to visual examination, while only the blend with $w_S = 0.20$ was investigated by SANS. Blends with $w_S = 0.10$ and 0.20 were examined by spectrophotometry. Carbon dioxide of >99.8%

* Author to whom correspondence should be addressed.
[†] North Carolina State University.
[‡] The Procter & Gamble Company.
[§] Oak Ridge National Laboratory.
[||] Present address: Department of Chemical Engineering, University of Delaware, Newark, DE 19716.

10.1021/jp990551f CCC: $18.00
Published on Web 05/29/1999

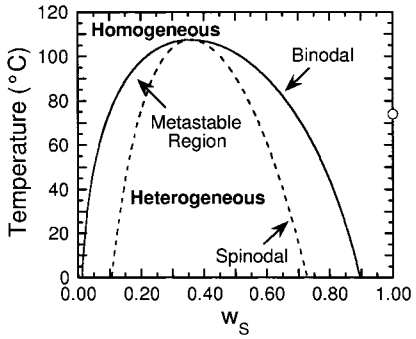

Figure 1. Predicted phase diagram for polystyrene ($\bar{M}_n = 3300$) and polyisoprene ($\bar{M}_n = 1000$) on the basis of the Flory−Huggins equation of state. Calculation of the binodal (coexistence) and spinodal (stability) curves as functions of composition (w_S) employs eqs 2 and 3 in the text, as well as the $\chi(T)$ expression reported in ref 27. The upper critical solution temperature (UCST) occurs at the intersection of the binodal and spinodal curves. The T_g of the PS employed in the blend (from DSC) is shown as (o).

purity and N_2 of >99.99% purity were obtained from National Specialty Gases (Durham, NC).

Methods. A high-pressure optical cell developed in-house was used for the visual experiments reported here. The interior dimensions of the cell were 15.9 mm × 15.9 mm × 6.4 mm, and the initial sample volume was approximately 0.75 cm^3. A thermocouple (Omega, type K) inserted into the cell (and immersed in the blend) recorded the blend temperature while the cell was heated. Carbon dioxide was fed into the cell using an ISCO syringe pump (260D) and pump controller (Series D) operated in constant pressure mode, and a pressure transducer (Omega PX302-10KGV) detected the pressure in the cell. Samples were allowed to homogenize quiescently at 100 °C for about 24 h upon initial cell loading, as well as after each pressure change. The temperature was varied at 0.5−2 °C/min, and resulting changes in isobaric phase behavior were recorded with either a Pulnix TN-7 CCD camera or a Shimadzu UV-265 spectrophotometer (operated at a wavelength of 700 nm). Visual experiments were repeated with the 20 wt % PS blend using N_2 instead of $scCO_2$. Measurements were initially acquired 15 min after pressurizing to minimize the extent of N_2 dissolution. Once the hydrostatic pressure was found to have little influence on T^*, measurements were collected after a 24-hr equilibration period to ascertain the effect of solubilized N_2 on T^*.

Phase-separation temperatures were also measured on the W. C. Koehler 30 m SANS facility[19] at Oak Ridge National Laboratory with a 64 × 64 cm^2 area detector and a cell (element) size of about 1 cm^2. The neutron wavelength (λ) was 0.475 nm ($\Delta\lambda/\lambda \sim 5\%$), and the sample-to-detector distance was 10 m. The data were corrected for instrumental background and detector efficiency on a cell-by-cell basis prior to radial averaging to yield a q range of $0.06 < q < 0.5$ nm^{-1}, where q denotes the scattering vector defined by $(4\pi/\lambda)\sin(\theta/2)$ (θ is the scattering angle). The net intensities were converted to an absolute (±5%) differential cross-section per unit sample volume (in units of cm^{-1}) by comparison with precalibrated secondary standards.[20] Experiments without CO_2 were conducted on a sample measuring about 1 cm in diameter and 1.5 mm thick and housed in a metal cell with removable quartz windows. For experiments with $scCO_2$, a high-pressure cell described in detail elsewhere[21−25] was employed. The samples were allowed to (i) homogenize for less than 1 h at 115 °C after the initial loading, as well as after the pressure change, and (ii) equilibrate for 25 min after each temperature increment (5 °C increments without $scCO_2$ and variable increments with $scCO_2$).

Results and Discussion

Displayed in Figure 1 is the theoretical phase diagram for the present PS−PI polymer blend, constructed on the basis of the Flory−Huggins equation of state:[26]

$$\frac{\Delta G_{mix}}{kT} = \frac{\phi_S \ln \phi_S}{\upsilon_S N_S} + \frac{\phi_I \ln \phi_I}{\upsilon_I N_I} + \frac{\chi \phi_S \phi_I}{\upsilon_{ref}} \quad (1)$$

Here, ΔG_{mix} is the change in free energy density upon mixing, k is the Boltzmann constant, and T denotes absolute temperature. The terms ϕ_i, υ_i, and N_i represent the volume fraction, repeat-unit volume, and repeat-unit number/chain, respectively, of polymer i, where i = S (for PS) or I (for PI). Values of υ_i are tabulated,[3] and the reference volume (υ_{ref}) is taken as the mean of υ_I (0.136 nm^3) and υ_S (0.179 nm^3). In calculating the binodal and spinodal curves for this UCST blend, the temperature-dependent Flory−Huggins interaction parameter for PS and PI reported by Rizos et al.[27] ($\chi = -0.07 + 63/T$) has been used in an iterative procedure to solve the governing sets of nonlinear equations that establish both phase coexistence (binodal conditions) and phase stability (spinodal conditions), viz.,

$$\text{binodal: } \chi = \frac{\upsilon_{ref}}{2}\left(\frac{1}{\upsilon_S N_S \phi_S} + \frac{1}{\upsilon_I N_I \phi_I}\right) \quad (2)$$

$$\text{spinodal: } \ln\left(\frac{\phi'_S}{\phi''_S}\right) + (\phi''_S - \phi'_S)\left(1 - \frac{\upsilon_S N_S}{\upsilon_I N_I}\right) + \frac{\chi \upsilon_S N_S}{\upsilon_{ref}}(\phi'^2_I - \phi''^2_I) = 0 \quad (3a)$$

$$\ln\left(\frac{\phi'_I}{\phi''_I}\right) + (\phi'_S - \phi''_S)\left(1 - \frac{\upsilon_I N_I}{\upsilon_S N_S}\right) + \frac{\chi \upsilon_I N_I}{\upsilon_{ref}}(\phi'^2_S - \phi''^2_S) = 0 \quad (3b)$$

The phases that coexist along the spinodal boundary are designated by ′ and ″. For illustrative purposes here, we make the simplifying assumption that χ is dependent only on temperature and is independent of pressure, whereas experimental evidence provided by Janssen et al.[28] indicates that the pressure dependence of χ may be nonnegligible. As seen in this figure, the ambient-pressure UCST (corresponding to the intersection of the binodal and spinodal curves) is predicted to occur at $T = 107$ °C and $w_S = 0.36$. Recall that the composition of one of the blends investigated in this study coincides with this predicted critical composition, while the other (off-critical) blend compositions have been selected arbitrarily.

Snapshots revealing the phase behavior of the PS−PI blend with $w_S = 0.20$ at various temperatures with and without $scCO_2$ are presented in Figure 2. In the absence of $scCO_2$ (top image series in Figure 2), the blend appears optically transparent at high temperatures, signifying a homogeneous system. Upon cooling at ambient pressure, the sample becomes initially turbid at T^* and grows increasingly opaque as the temperature is lowered further. Values of T^* measured in this manner, as well as by spectrophotometry, are within 2 to 3 °C irrespective of whether they are measured during the heating or cooling cycles: $T^* \approx 98$ °C at $w_S = 0.36$ and $T^* \approx 84$ °C at $w_S = 0.20$. From spectrophotometry measurements (performed at a wavelength of 700 nm), $T^* \approx 83$ °C at $w_S = 0.20$. These measured values of T^* are below the predicted binodal points

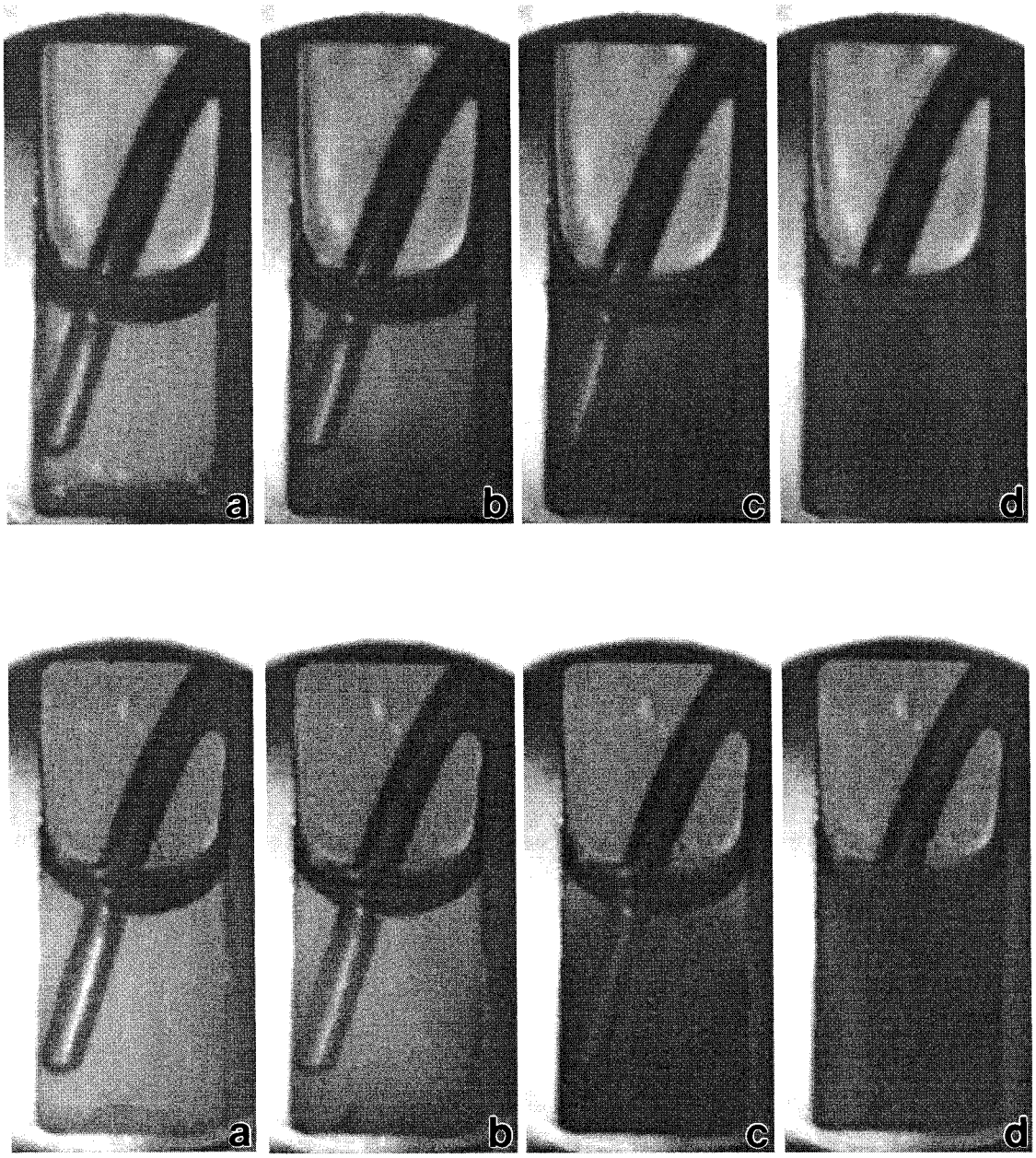

Figure 2. CCD image series of the PS−PI blend with $w_S = 0.20$ in the absence of $scCO_2$ (top) and presence of $scCO_2$ at 13.8 MPa (bottom). In the top image series, the temperatures (in °C) are (a) 87, (b) 83, (c) 81, and (d) 78, whereas those in the bottom series are (a) 58, (b) 56, (c) 56, and (d) 54. The cloud point (T^* at ambient pressure; T^*_p at elevated pressure) identifies the temperature at which the blend first appears turbid upon cooling from a homogeneous solution.

in Figure 1 (by about 10 °C), but above the glass transition temperature (T_g) of the PS (74 °C, according to differential scanning calorimetry, DSC). Visual experiments employing $scCO_2$ have been conducted at two pressures, 13.8 and 34.5 MPa, and are provided in the bottom image series in Figure 2 for the data obtained at 13.8 MPa. As in the nonsolvated blends, specimens sorbed with $scCO_2$ appear optically transparent at elevated temperatures and become cloudy upon decreasing the temperature below T^*_p (the subscript denotes a pressure above ambient). For the blend with $w_S = 0.20$, measured values of T^*_p are 56 °C at 13.8 MPa and 62 °C at 34.5 MPa. Results from the blend with $w_S = 0.36$ are comparable: values of T^*_p are 76 and 85 °C at 13.8 and 34.5 MPa, respectively. In both blends, addition of $scCO_2$ is found to promote a nontrivial reduction in the cloud point.

Figure 3 shows temperature-dependent SANS profiles for the PS−PI blend presented in Figure 2 ($w_S = 0.20$) without (Figure 3a) and with (Figure 3b) $scCO_2$. Phase separation in this nondeuterated blend is evidenced by an upturn in scattering intensity at low q (i.e., at large spatial dimensions). In the absence of $scCO_2$, an unambiguous upturn is first noticed between 65 and 70 °C (see Figure 3a), which is somewhat lower than the T^* measured visually and predicted theoretically. Once the sample is subjected to $scCO_2$ at 14.5 MPa in accord with the conditions described earlier, the initial upturn in scattering intensity at low q is seen in Figure 3b to shift to 40−43 °C, confirming that $scCO_2$ depresses the cloud point of the blend. As above, the value of T^*_p measured by SANS is lower than that determined visually. The differing cloud point temperatures discerned from visual and scattering methods (due to differences in the length scale probed in each) are not, however, the focus of this study. Instead, we draw attention to the apparent $scCO_2$-induced reduction in the cloud point. This cloud point depression, denoted ΔT^* ($= T^*_p - T^*$), is presented as a function of

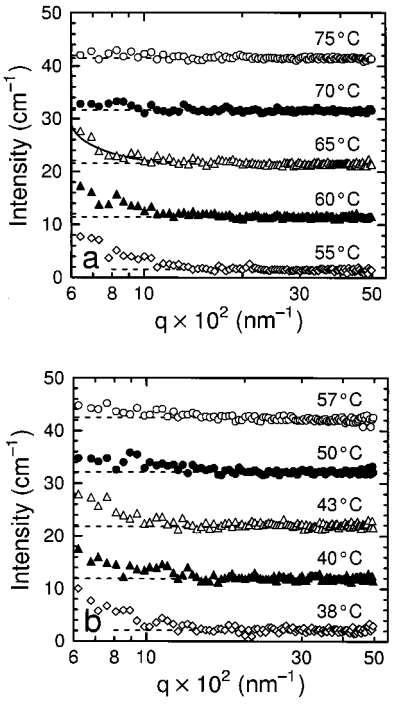

Figure 3. SANS profiles collected from the PS−PI blend with $w_S = 0.20$ in the (a) absence of $scCO_2$ and (b) presence of $scCO_2$ at 14.5 MPa. Each profile is labeled with the corresponding temperature. The onset of phase separation in the blend is accompanied by an upturn in intensity at low q, as illustrated by the solid curve in (a) and deviation from the horizontal dashed lines in (a) and (b). These profiles are shifted vertically to facilitate discrimination.

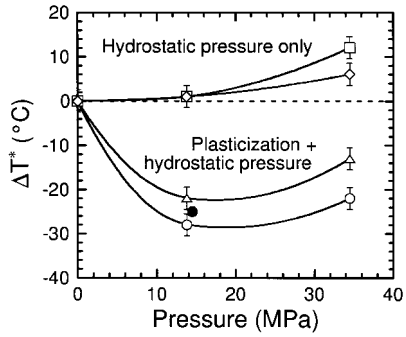

Figure 4. Dependence of ΔT^* on pressure for PS−PI blends differing in composition (w_S): 0.20, in $scCO_2$ (circles); 0.20, in N_2 (diamonds, squares); and 0.36, in $scCO_2$ (triangles). Specimens examined visually are denoted by open symbols, whereas those investigated by SANS are indicated by filled symbols. Samples exposed to N_2 have been equilibrated for 15 min (diamonds) and 24 h (squares), while those exposed to $scCO_2$ have all been equilibrated for 24 h prior to measurement. The solid lines serve as guides for the eye.

pressure in Figure 4 and reveals that $scCO_2$ induces the most significant reduction in phase-separation temperature (22−28 °C) in the off-critical blend possessing $w_S = 0.20$. In the critical blend with $w_S = 0.36$, ΔT^* ranges from 13 to 22 °C.

In Figure 4, ΔT^* is consistently the most negative at the lower $scCO_2$ pressure (13.8 MPa) and then increases (decreases in magnitude) as the pressure is increased to 34.5 MPa in both blends. To elucidate the meaning of this behavior and delineate the effects of plasticization and hydrostatic pressure, additional experiments have been performed on the $w_S = 0.20$ blend in the presence of high-pressure N_2. Values of T^* measured from blends composed of both filtered and unfiltered PI prior to addition of N_2 and after decompression are identical within ±1 °C. This observation, coupled with reported[29] data indicating

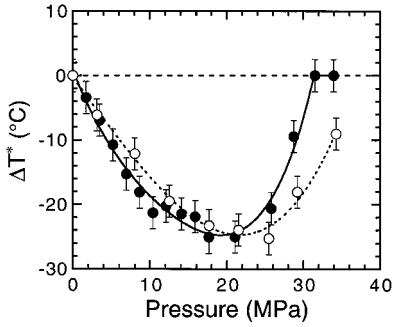

Figure 5. Variation of ΔT^* with $scCO_2$ pressure for PS−PI blends differing in composition (w_S): 0.10 (●) and 0.20 (○). The solid and dotted lines serve as guides for the eye for the blends with $w_S = 0.10$ and $w_S = 0.20$, respectively, and the vertical lines denote the experimental uncertainty inherent in the data (±2.5 °C).

that the solubility of N_2 in polystyrene is about an order of magnitude less than that of CO_2, confirms that polymer plasticization due to N_2 can, at short exposure times, be considered negligible. Measured values of T^*_p in the presence of N_2 are 85 °C at 13.8 MPa and 90 °C at 34.5 MPa. Corresponding values of ΔT^* are +1 and +6 °C, respectively. At a longer (24-hr) equilibration time, the value of ΔT^* at 34.5 MPa increases further to +12 °C. These results are in favorable agreement with those of recent studies[30−33] investigating UCST blends and block copolymers at high hydrostatic pressure. Such studies report that an increase in pressure is generally accompanied by a reduction in the homogeneous temperature range (and an increase in T^*_p).

The data compiled in Figure 4 reveal that the plasticization efficacy of $scCO_2$, rather than the corresponding hydrostatic pressure, is responsible for the observed reduction in T^* ($\Delta T^* < 0$). In light of the results from the complementary N_2 experiments and assuming a relatively small experimental error, we also attribute the decrease in the magnitude of ΔT^* at 34.5 MPa to the increased hydrostatic pressure. Thus, the plasticization efficacy of $scCO_2$, which increases the free volume of a molten polymer[18] and depresses T_g in glassy polymers,[17] competes with the condensing (or "freezing-in") effect of hydrostatic pressure,[34] indicating that an optimum pressure yielding a minimum ΔT^* must exist (qualitatively shown by the solid line in Figure 4). This optimum pressure is unambiguously evident in the pressure-dependent ΔT^* data collected by spectrophotometry and presented in Figure 5 for PS−PI blends with $w_S = 0.10$ and $w_S = 0.20$. At these blend compositions, the optimum pressure is observed to occur in the vicinity of 20 ± 2 MPa. It should be recognized that, while all the temperatures at which cloud points were measured lie above the critical temperature of CO_2 (31 °C), *not* all the pressures in Figure 5 exceed the critical pressure of CO_2 (7.4 MPa). Thus, we find that CO_2 as either a high-pressure gas or a supercritical fluid can influence (and, in the present UCST system, enhance) the mixing efficacy of macromolecules.

Conclusions

This study clearly demonstrates that the homogeneous regime of a blend composed of PS and PI can be controllably increased through the addition of $scCO_2$. Moreover, the effect of $scCO_2$ on PS−PI blend phase behavior (characterized by the cloud point) is not monotonic in pressure, since hydrostatic effects become increasingly important, and cannot be neglected, as the pressure is increased. An optimum $scCO_2$ pressure corresponding to a maximum in cloud point depression has consequently

been identified. While the present work employs model short-chain polymers, the results obtained here may apply to high-molecular-weight commercial blends with a low χ (which can homogenize before decomposing). In this event, which is currently under investigation, effective use of $scCO_2$ as an environmentally benign diluent for the improved processing of polymer blends would most likely be viable at low to moderate pressures above the critical point of CO_2.

Acknowledgment. We gratefully acknowledge support from the Kenan Center for the Utilization of Carbon Dioxide in Manufacturing at North Carolina State University and the University of North Carolina at Chapel Hill. Work performed at Oak Ridge National Laboratory was supported by the Division of Advanced Energy Projects, Materials and Chemical Sciences, U.S. Department of Energy under Contract No. DE-AC05-96OR22464 with Lockheed Martin Energy Research Corporation. We also thank Ms. Jennifer Shay for assistance with the GPC measurements.

References and Notes

(1) Bates, F. S. *Science* **1991**, *251*, 898.
(2) Binder, K. *Adv. Polym. Sci.* **1994**, *112*, 181.
(3) Balsara, N. P. In *Physical Properties of Polymers Handbook*; Mark, J. E., Ed.; AIP Press: New York, 1996; Chapter 19.
(4) Coleman, M. M.; Painter, P. C. *Prog. Polym. Sci.* **1995**, *20*, 1.
(5) Watkins, J. J.; McCarthy, T. J. *Macromolecules* **1995**, *28*, 4067.
(6) Cooper, A. I.; DeSimone, J. M. *Curr. Opin. Solid State Mater. Sci.* **1996**, *1*, 761.
(7) Kerton, F. M.; Lawless, G. A.; Armes, S. P. *J. Mater. Chem.* **1997**, *7*, 1965.
(8) Beaucage, G.; Aubert, J. H.; Lagasse, R. R.; Schaefer, D. W.; Rieker, T. P.; Erlich, P.; Stein, R. S.; Kulkarni, S.; Whaley, P. D. *J. Polym. Sci. B: Polym. Phys.* **1996**, *34*, 3063.
(9) Mawson, S.; Johnston, K. P.; Betts, D. E.; McClain, J. B.; DeSimone, J. M. *Macromolecules* **1997**, *30*, 71.
(10) Mawson, S.; Kanakia, S.; Johnston, K. P. *Polymer* **1997**, *38*, 2957.
(11) Watkins, J. J.; Brown, G. D.; Pollard, M. A.; Ramachandra-Rao, V.; Russell, T. P. *Polym. Mater. Sci. Eng.* **1998**, *78*, 94.
(12) Bungert, B.; Sadowski, G.; Arlt, W. *Fluid Phase Equil.* **1997**, *139*, 349.
(13) Frielinghaus, H.; Schwahn, D.; Mortensen, K.; Willner, L.; Almdal, K. *J. Appl. Crystallogr.* **1997**, *30*, 696.
(14) Maeda, Y.; Karasz, F. E.; MacKnight, W. J. *J. Polym. Sci., Polym. Phys. Ed.* **1986**, *24*, 2345.
(15) Sefcik, M. D. *J. Polym. Sci., Polym. Phys. Ed.* **1986**, *24*, 957.
(16) Li, M.; Bright, F. V. *Appl. Spectrosc.* **1996**, *50*, 740.
(17) Shieh, Y. T.; Su, J. H.; Manivannan, G.; Lee, P. H. C.; Sawan, S. P.; Spall, W. D. *J. Appl. Polym. Sci.* **1996**, *59*, 707.
(18) Gerhardt, L. J.; Garg, A.; Manke, C. W.; Gulari, E. *J. Polym. Sci. B: Polym. Phys.* **1998**, *36*, 1911.
(19) Koehler, W. C. *Physica (Utrecht)* **1986**, *137B*, 320.
(20) Wignall, G. D.; Bates, F. S. *J. Appl. Crystallogr.* **1986**, *20*, 28.
(21) Guan, Z.; DeSimone, J. M. *Macromolecules* **1994**, *27*, 5527.
(22) McClain, J. B.; Londono, J. D.; Romack, T. J.; Canelas, D. P.; Betts, D. E.; Wignall, G. D.; Samulski, E. T.; DeSimone, J. M. *J. Am. Chem. Soc.* **1996**, *118*, 917.
(23) Canelas, D. A.; Betts, D. E.; DeSimone, J. M. *Macromolecules* **1996**, *29*, 2818.
(24) McClain, J. B.; Londono, J. D.; Chillura-Martino, D.; Triolo, R. T.; Betts, D. E.; Samulski, E. T.; Wignall, G. D.; DeSimone, J. M. *Science* **1996**, *274*, 2049.
(25) Londono, J. D.; Dharmapurikar, R.; Cochran, H. D.; Wignall, G. D.; McClain, J. B.; Betts, D. E.; Canelas, D.; DeSimone, J. M.; Samulski, E. T.; Chillura-Martino, D.; Triolo, R. *J. Appl. Crystallogr.* **1997**, *30*, 690.
(26) Huggins, M. L. *J. Chem. Phys.* **1941**, *9*, 440. Flory, P. J. *J. Chem. Phys.* **1941**, *9*, 660. See also Scott, R. L. *J. Polym. Sci.* **1952**, *9*, 423.
(27) Rizos, A. K.; Fytas, G.; Semenov, A. N. *J. Chem. Phys.* **1995**, *102*, 6931.
(28) Janssen, S.; Schwahn, D.; Springer, T.; Mortensen, K.; Hasegawa, H. *Physica B* **1995**, *213*, 691.
(29) Sato, Y.; Yurugi, M.; Fujiwara, K.; Takishima, S.; Masuoka, H. *Fluid Phase Equil.* **1996**, *125*, 129.
(30) Hajduk, D. A.; Gruner, S. M.; Shyamsunder, E.; Register, R. A.; Fetters, L. J. *Macromolecules* **1996**, *29*, 1473.
(31) Kojima, J.; Nakayama, Y.; Takenaka, M.; Hashimoto, T. *Rev. Sci. Instrum.* **1995**, *66*, 4066.
(32) Xiong, Y.; Kiran, E. *Rev. Sci. Instrum.* **1998**, *69*, 1463.
(33) Frielinghaus, H.; Schwahn, D.; Mortensen, K.; Willner, L.; Almdal, K. *Physica B* **1997**, *234*−*236*, 260.
(34) Condo, P. D.; Sanchez, I. C.; Panayiotou, C. G.; Johnston, K. P. *Macromolecules* **1992**, *25*, 6119.